Support Information

Origin of the Enantioselectivity of Alcohol Dehydrogenase

Jiahui Zhou[1#], Tao Han[2#], Shahbaz Ahmad[1,3], Derek Quinn[3], Thomas Moody[3,4], Qi Wu[2]*,

Meilan Huang[1]*

[1] School of Chemistry and Chemical Engineering, Queen's University, David Keir Building,

Stranmillis Road, Belfast BT9 5AG, Northern Ireland, UK;

[2] Department of Chemistry, Zhejiang University, Hangzhou, 310027, P. R. China;

[3] Almac Sciences, Department of Biocatalysis and Isotope Chemistry, Almac House, 20

Seagoe Industrial Estate, Craigavon BT63 5QD, Northern Ireland, United Kingdom;

[4] Arran Chemical Company Limited, Unit 1 Monksland Industrial Estate, Athlone,

Co. Roscommon, Ireland

[#] Equal contributions

Figure S1. Representation of the QM and MM regions in the QM/MM calculations (a) QM and MM division. The QM atoms are shown in sticks and the MM atoms are shown in lines. (b) atoms included in the QM calculations.
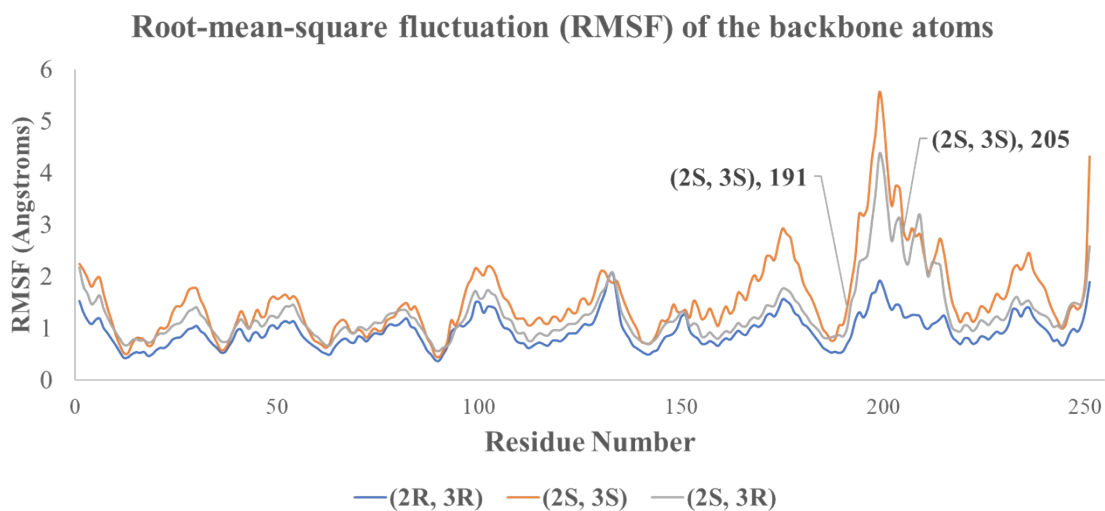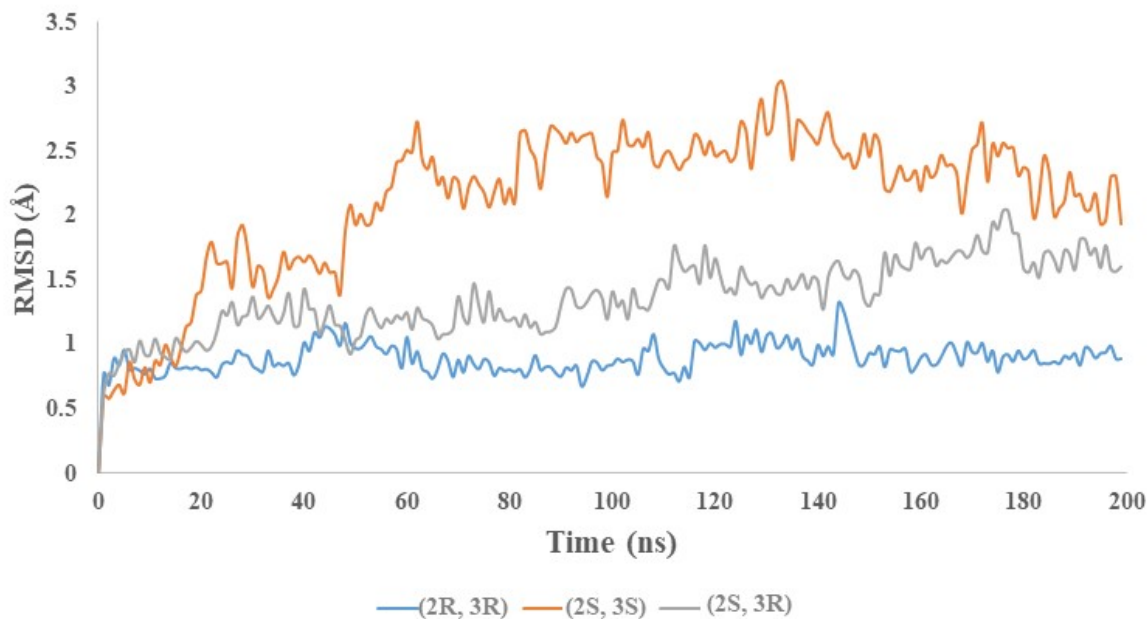
(a)

(b)

Figure S2. (A) RMSD plot of *Lb*ADH in complex with the substrate poses that lead to the major product (*2R, 3R*) (in blue), the minor product (*2S,3S*) (in orange) and the inaccessible product (*2S, 3R*) (in grey). (B) RMSF plot of the protein backbone atoms of the enzyme in complex with the substrate poses that lead to the major product (*2R, 3R*) (in blue), the minor product (*2S,3S*) (in orange) and the inaccessible product (*2S, 3R*) (in grey).
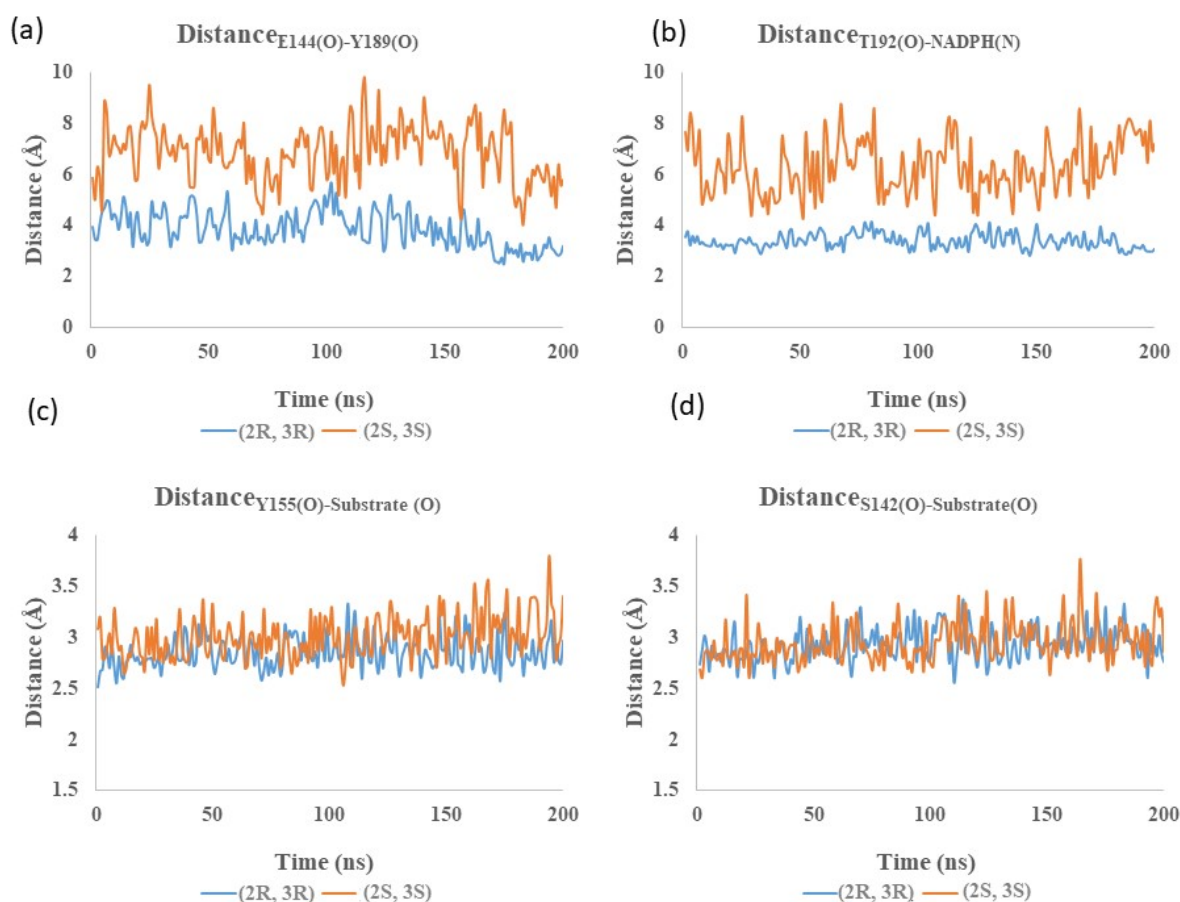
Figure S3. The distances between the substrate and the ADH enzyme from MD simulations. (A) Distance between Glu144 and Tyr189 indicates the presence of hydrogen bond in the major product (*2R, 3R*) and the absence of the hydrogen bond in the minor product (*2S,3S*); (B) Distance between Thr192 oxygen and NADPH nitrogen indicates the presence of hydrogen bond in the major product (*2R, 3R*) and the absence of the hydrogen bond in the minor product (*2S,3S*); (C) Distance between Tyr155 and the substrate carbonyl oxygen indicates the formation of stable hydrogen bonds; (D) Distance between Ser142 and the substrate carbonyl oxygen indicates the formation of stable hydrogen bonds.
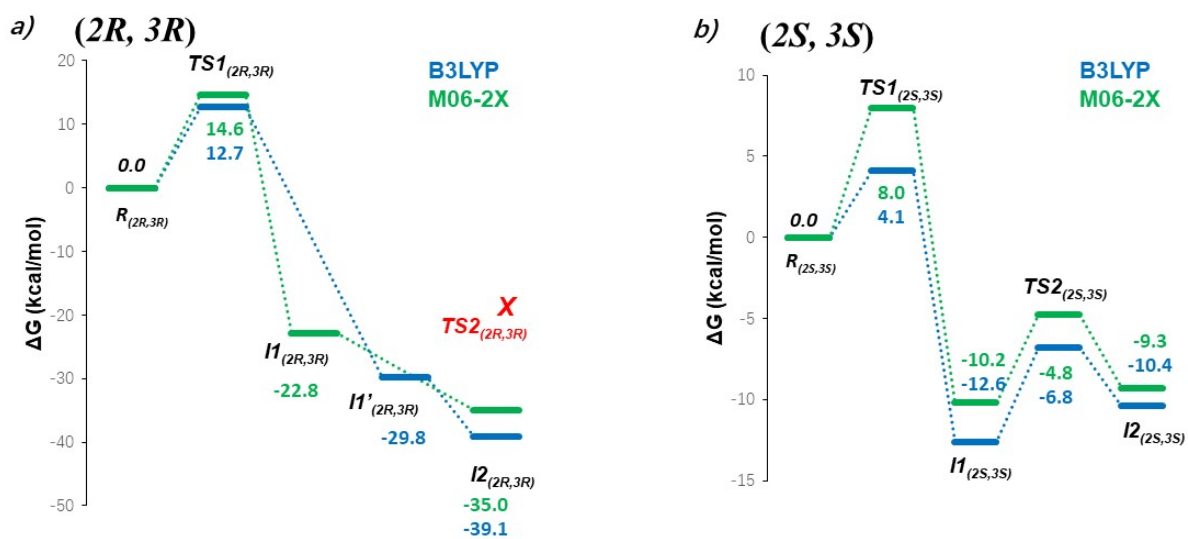
Figure S4. Free energy profile for (A) the major product (*2R, 3R*) and (B) the minor product (*2S,3S*). Geometries were optimized at B3LYP and M06-2X with the 6-31G* basis set.
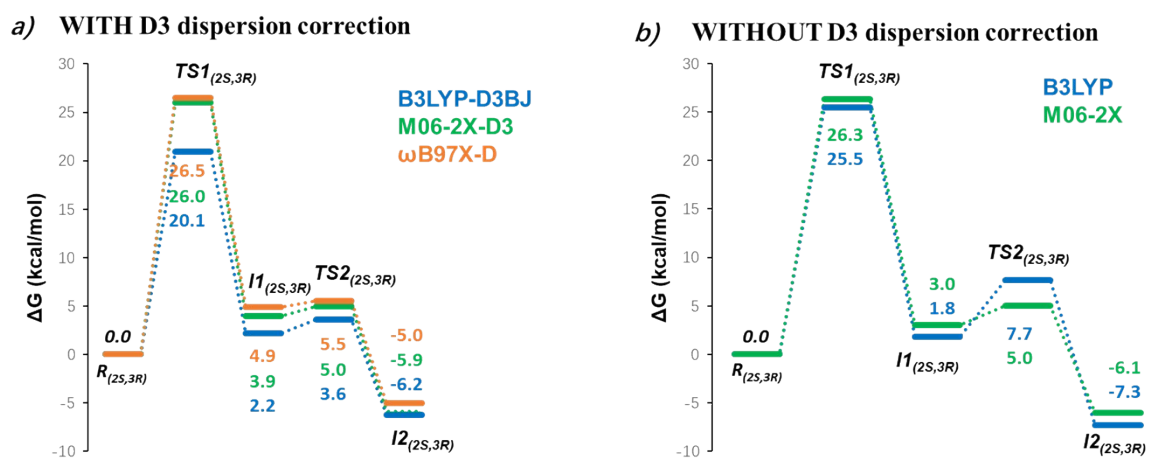
Figure S5. Free Energy Profile of the inaccessible product (*2S,3R*). (A) Geometries were optimized at B3LYP-D3(BJ), M06-2X-D3 and ωB97X-D with the 6-31G* basis set. (B) Geometries were optimized at B3LYP and M06-2X with the 6-31G* basis set.
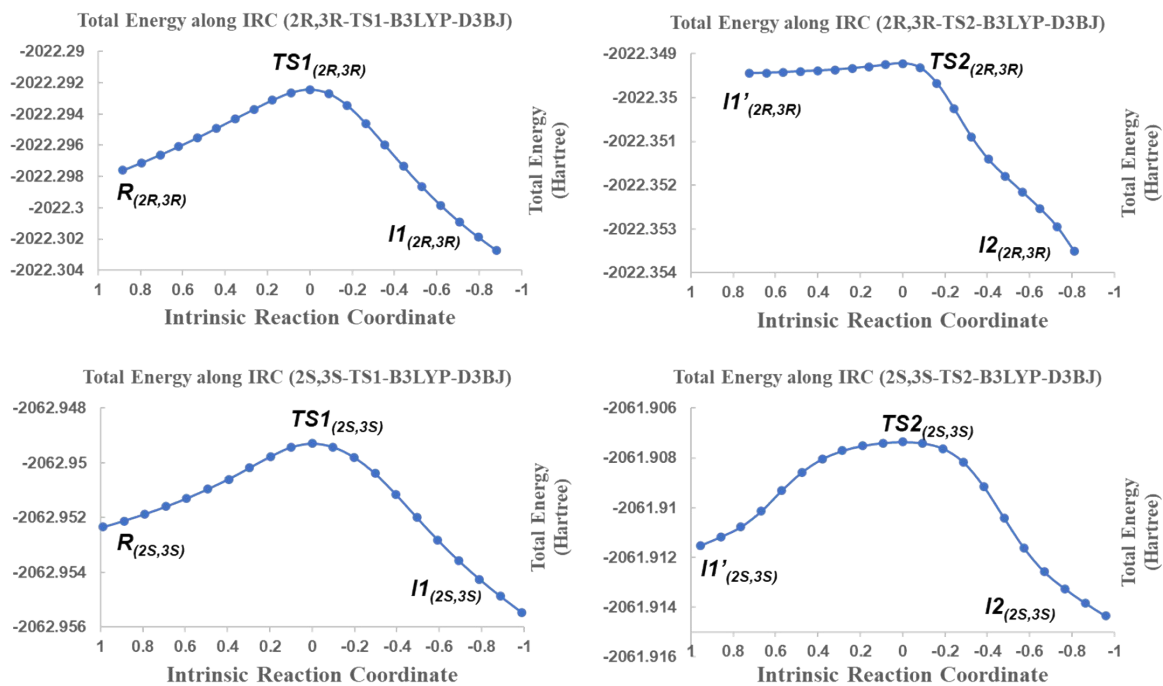
Figure S6. IRC analysis for the two transition states TS1 and TS2 in the major product (*2R, 3R*) and the minor product (*2S,3S*).
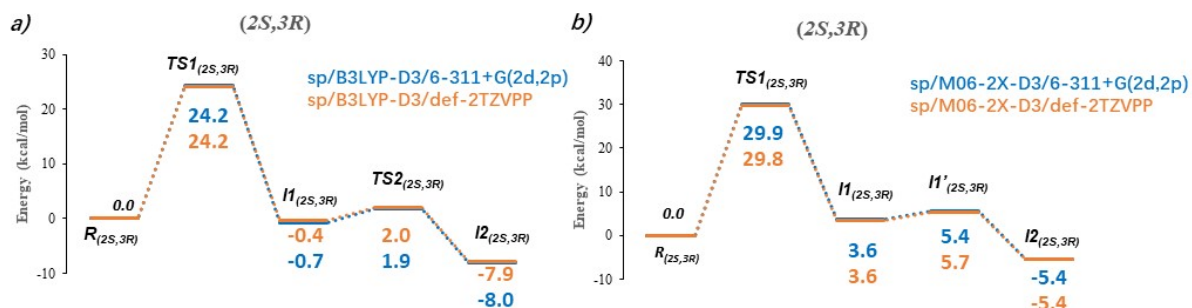
Figure S7. Free energy profile for the enzyme-substrate complexes with the substrate poses leading to the inaccessible product (2S, 3R). Single point energy corrections were conducted with large basis sets 6-311+G(2d,2p) and def-2TZVPP based on the optimized geometries obtained at (A) B3LYP-D3(BJ)/6-31G* and (B) M06-2X-D3/6-31G*.
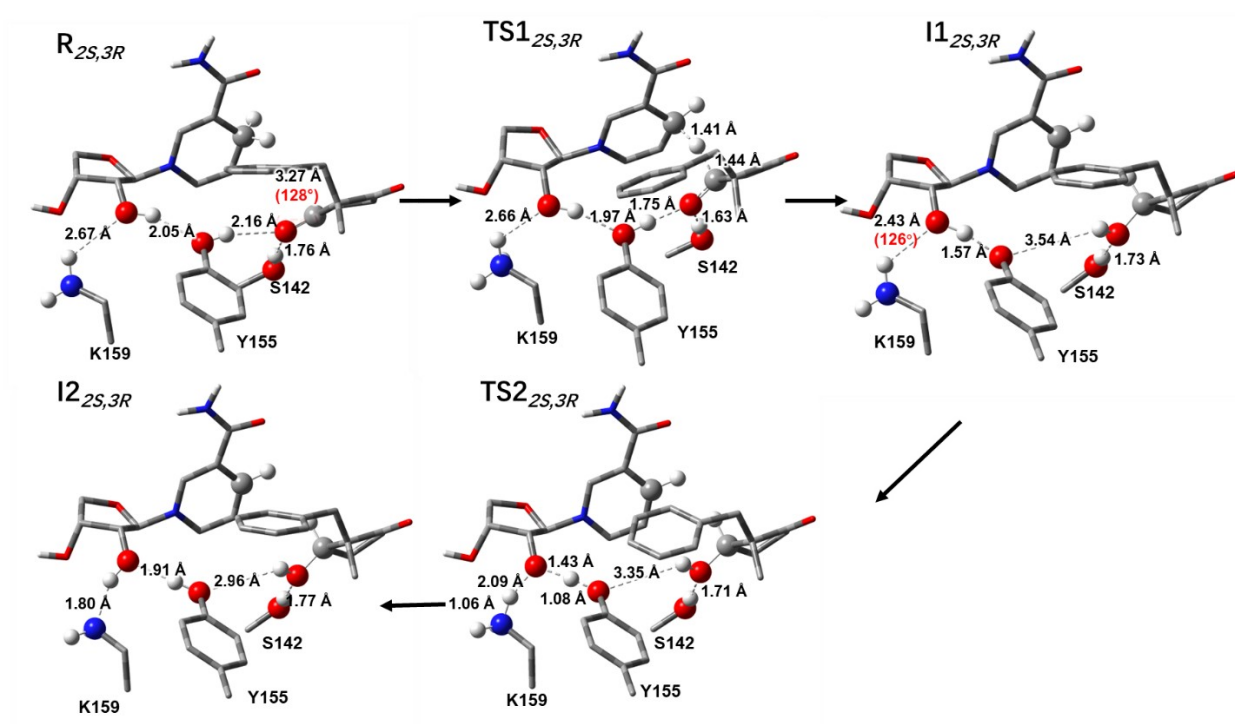
Figure S8. Optimized structures of the inaccessible product (*2S,3R*). Geometries were optimized at B3LYP-D3(BJ) funtional level with the 6-31G* basis set.
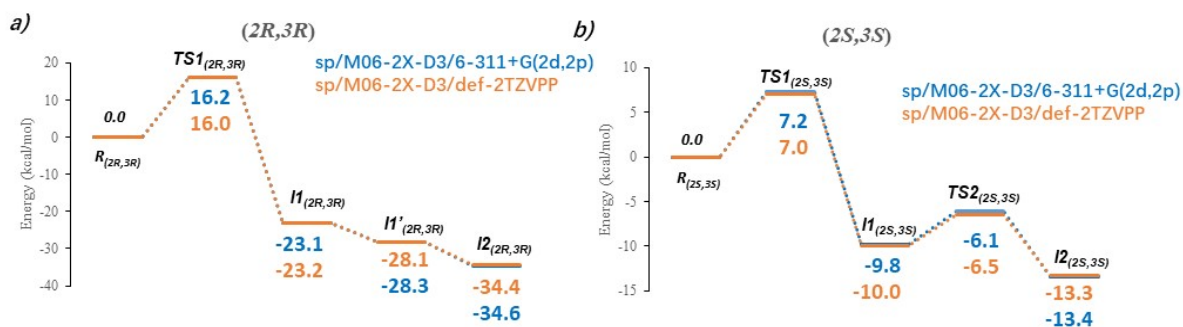
Figure S9. Free energy profile for the enzyme-substrate complexes with the substrate poses leading to (A) (*2R, 3R*) or (B) (*2S, 3S*) product. Single point energy corrections were conducted with large basis sets 6-311+G(2d,2p) and def-2TZVPP based on the optimized geometries obtained at M06-2X-D3/6-31G*.